

In Vivo Calcium Imaging of Granule Cells in the Dentate Gyrus of Hippocampus in Mice

Shanshan Han¹, Ning Ding¹, Ce Li¹, Peng Yuan¹

¹ Department of Rehabilitation Medicine, Huashan Hospital, State Key Laboratory of Medical Neurobiology, Institute for Translational Brain Research, MOE Frontiers Center for Brain Science, MOE Innovative Center for New Drug Development of Immune Inflammatory Diseases, Fudan University

Corresponding Author

Peng Yuan

pyuan@fudan.edu.cn

Citation

Han, S., Ding, N., Li, C., Yuan, P. *In Vivo Calcium Imaging of Granule Cells in the Dentate Gyrus of Hippocampus in Mice*. *J. Vis. Exp.* (210), e66916, doi:10.3791/66916 (2024).

Date Published

August 2, 2024

DOI

10.3791/66916

URL

jove.com/video/66916

Abstract

Real-time approaches are typically needed in studies of learning and memory, and *in vivo* calcium imaging provides the possibility to investigate neuronal activity in awake animals during behavior tasks. Since the hippocampus is closely associated with episodic and spatial memory, it has become an essential brain region in this field's research. In recent research, engram cells and place cells were studied by recording the neural activities in the hippocampal CA1 region using the miniature microscope in mice while performing behavioral tasks including open-field and linear track. Although the dentate gyrus is another important region in the hippocampus, it has rarely been studied with *in vivo* imaging due to its greater depth and difficulty for imaging. In this protocol, we present in detail a calcium imaging process, including how to inject the virus, implant a GRIN (Gradient-index) lens, and attach a base plate for imaging the dentate gyrus of the hippocampus. We further describe how to preprocess the calcium imaging data using MATLAB. Additionally, studies of other deep brain regions that require imaging may benefit from this method.

Introduction

Previous studies found that the hippocampus is a brain structure essential for processing and retrieving memories^{1,2}. Since the 1950s, the neural circuits of the hippocampus in rodents have been a focus in studying memory formation, storage, and retrieval³. The anatomical structures within the hippocampus include the subregions of dentate gyrus (DG), CA1, CA2, CA3, CA4, and subiculum⁴. Complex bidirectional connections exist among these subregions, of which the DG, CA1, and CA3 form

a prominent trisynaptic circuit that consists of granule cells and pyramidal cells⁵. This circuit receives its primary input from the entorhinal cortex (EC) and has been a classic model for studying synaptic plasticity. Prior *in vivo* research on the hippocampus function has mostly concentrated on the CA1^{6,7} due to its easier access. While CA1 neurons serve important roles in memory formation, consolidation, and retrieval, particularly in place cells for spatial memory, other subregions of the hippocampus are also vital^{8,9}. In particular,

recent studies have highlighted the functions of DG in memory formation. Place cells in DG have been reported to be more stable than those in CA1¹⁰, and their activities reflect context-specific information¹¹. Further, activity-dependent labeling of DG granule cells can be reactivated to induce memory-related behaviors¹². Therefore, to gain a deeper understanding of the information coding in DG, it is crucial to investigate the activities of the DG subregion while the animal is carrying out memory-dependent tasks.

Prior studies of DG activities have mostly used *in vivo* electrophysiology¹³. However, this technique has some drawbacks: First, in electrical recordings, it may be difficult to directly identify the various types of cells that are generating the signal. The recorded signals are from both inhibitory and excitatory cells. Therefore, further data processing methods are required to separate these two cell types. Moreover, it is difficult to combine other cell type information, such as projection-specific subgroups or activity-dependent labeling, with electric recordings. In addition, due to the anatomical morphology of DG, the recording electrodes are often implanted in an orthogonal direction, which greatly limits the number of neurons that can be recorded. Thus, it is difficult for electric recordings to achieve monitoring hundreds of individual neurons from the DG structure in the same animal¹⁴.

A complementary technique of recording neuron activities in DG is to use *in vivo* calcium imaging¹⁵. Calcium ions are fundamental to cellular signaling processes in organisms, playing a crucial role in many physiological functions, especially within the mammalian nervous system. When neurons are active, the intracellular calcium concentration increases rapidly, reflecting the dynamic nature of neuronal activity and signal transmission. Therefore, recording

the real-time changes in intracellular calcium levels in neurons provides important insights into the neural coding mechanisms.

Calcium imaging technology utilizes specialized fluorescent dyes or genetically engineered calcium indicators (GECIs) to monitor calcium ion concentrations in neurons by detecting changes in fluorescence intensity, which can then be captured through microscopic imaging¹⁶. Commonly, the GCaMP family of calcium indicator genes, comprising green fluorescent protein (GFP), calmodulin, and M13 polypeptide sequences, are employed. GCaMP can emit green fluorescence when it binds to calcium ions¹⁷, allowing the fluctuations in green fluorescence to be recorded via imaging¹⁸. Additionally, to obtain clear images of the target brain region, a Gradient Index Lens (GRIN lens) is typically implanted above the region of interest. The GRIN lens enables imaging of the deep brain region that cannot be accessed directly from the surface.

This technique is relatively easy to combine with other genetic tools to label different cell types. Moreover, as the imaging plane is parallel to the cells' orientation in DG, hundreds of neurons are accessible for imaging with each successful surgery. In this work, we present a complete and detailed surgery protocol for *in vivo* calcium imaging in the dentate gyrus in mice (**Figure 1**). The procedure involves two major operations. The first one is to inject the AAV-CaMKII α -GCaMP6f virus into the DG. The second operation is to implant a GRIN lens above the virus injection site. These two procedures are conducted in the same sitting. After recovery from these surgeries, the next step is to check the imaging quality with miniaturized microscopes (miniscopes). If the imaging field has hundreds of active cells, the subsequent procedure is to attach the miniscope base plate onto the

mouse skull using dental cement; the mouse can then be used for imaging experiments. We also present a MATLAB-based preprocessing pipeline for streamlining the analysis of the collected calcium data.

Protocol

All the animal procedures were approved by the Institutional Animal Care and Use Committee at Fudan University (202109004S). All animals used in this study were 6-month-old C57BL/6J; both sexes were used. Mice were kept on a 12 h light cycle, from 8 AM to 8 PM. We used the following coordinates for virus injection in DG: A/P: -2.2 mm, M/L: 1.5 mm, D/V: 1.7 mm from the brain surface.

1. Virus injection into the dentate gyrus

1. Wear protective equipment, including single-use sterile gloves and gowns.
2. Prepare the required surgical instruments, two tubes of 5 mL of saline (0.9% NaCl [sterile] or artificial cerebrospinal fluids) and two 25 G luer lock blunt needles.
NOTE: All surgical instruments must be thoroughly sterilized prior to the operation. We used autoclaving at high temperature (121-134 °C) and pressure (20 psi) to sterilize the surgical instruments. Furthermore, we sprayed the surfaces with alcohol-based disinfectants. In all surgical procedures, we utilized 0.9% sterile saline solution. Instruments were intermittently sterilized during surgery with heated glass beads.
3. Prepare a 10% bleach solution in water to disinfect any supplies that may come into contact with the virus.
4. Dilute the AAV-CaMKII α -GCaMP6f virus if necessary, using sterilized saline, and store it in the 4 °C refrigerator

or on ice. The target final titer of the virus is 1×10^{12} GC/mL.

NOTE: We recommend avoiding repeated freeze-thaw cycles of the virus to preserve virus integrity. To this end, we generally aliquot the virus when received from the manufacturer into small volumes (e.g., 2 μ L per tube) and keep them in a -80 °C freezer. Virus should be used on the day of thawing and should not be stored at 4 °C for long-term use.

5. Use a micropipette puller to pull the micropipette to a fine tip, snip off a little portion of the tip with surgical scissors, and fill the tube with mineral oil. Ensure the pipette can suck liquid normally and then, install it on the injector.
NOTE: We used a one-step pulling method with the heater set at ~60% of the maximal power. Other pullers may be used for this step. The overall goal is to make the tip ~50-100 μ m in diameter; too small a diameter will affect the flow of the liquid; too thick may cause damage to the brain tissue of the mouse.
6. Turn on all instruments, including the mouse anesthesia machine, temperature maintenance machine (heating pad), and vacuum pump. In addition, measure the body weight of the mice before the surgery.
NOTE: During the procedure, we monitored the breathing of the mouse visually and occasionally checked the body temperature to ensure they were in good condition.
7. Place the mouse in the gas chamber with 2.5% isoflurane and 1 L of Oxygen/min. Monitor the breathing conditions of the mouse to gauge the anesthesia status.
NOTE: The respiratory rate should be about 1 breath/s to keep the mouse in good health.
8. Take the mouse out of the gas chamber and place it on the stereotaxic apparatus.

9. Ensure the mouse is adequately anesthetized before starting the next operation. Test the pedal withdrawal reflex by pinching the foot pads of both hind feet. If the mouse responds to the foot pad pinch, administer additional anesthesia and re-test the reflex before proceeding.

10. Cover the mouse nose with a mask and set the isoflurane flow rate to 1.5%. Fix the mouse head firmly with ear bars (**Figure 2A**).

NOTE: Be careful not to fix the ear bars too tightly on the mouse since this could easily affect the breathing of the mouse and in some cases, cause death.

11. Trim the top of the mouse's head with surgical scissors, and use depilatory cream to remove any leftover hair until the skin is completely exposed. Apply the depilatory cream to the scalp of the mouse, let it sit for approximately 5 min, and use gauze to wipe the cream off.

12. Apply ophthalmic ointment on the mouse's eyes.

13. Disinfect the hairless area with iodophor disinfectant and 75% ethanol using cotton swabs.

14. Make a continuous incision along the midline of the scalp using surgical scissors (or a scalpel blade), and cut off part of the scalp to expose the skull surface (**Figure 2B**). Rinse the surface of the skull with saline; then, remove the fascia and excessive saline using a vacuum pump. Repeat this process multiple times until the area around the wound stops bleeding. Wipe the surface of the skull with cotton swabs to keep it dry.

NOTE: There are other ways to remove the fascia, such as wiping it away with a cotton ball or cotton swab.

15. Use the locating needle to adjust the cranial surface when the bregma and lambda are visible. Make several

adjustments until the entire head is leveled (the entire error in the Z-axis direction is less than 0.05 mm).

16. Move the tip of the needle from the bregma to the appropriate target position. For the target coordinates, use the bregma as the reference point. Mark the four points to define the perimeter of the virus injection site: A/P: -2.0 mm, M/L: -1.5 mm; A/P: -2.5 mm, M/L: -1.5 mm; A/P -2.25 mm, M/L: -1.0 mm; and A/P -2.25 mm, M/L: -2.0 mm, with an erasable marker.

NOTE: This protocol performs the virus injection and GRIN lens implantation in the same surgery. In this protocol, all surgeries were performed on the right hemisphere, but it is conceivable that either hemisphere can be used. Within the injection area defined by the four points mentioned above, inject the virus in three separate 80 nL doses at different locations. Although the three locations were chosen arbitrarily, we recommend that they be dispersed for better virus spread. This will increase the number of infected cells.

17. Make the craniotomy in the region with the microdrill and set these four points as the border. Stop drilling when brain tissue is visible (**Figure 2C**).

NOTE: Try to drill the skull slowly. The drill bit may harm the brain tissue due to excessive force. Slow drilling can also prevent overheating of the brain.

18. Remove the bone debris and dura using ultra fine forceps and constantly rinse this area with sterile saline.

NOTE: It is normal for a small amount of bleeding to occur during this step, as some capillaries rupture; just keep rinsing with saline until there is no more bleeding.

19. Use the control panel of the injector to eject some mineral oil to generate the required space for the subsequent

loading of the virus. Fill the micropipette with at least 240 nL of the diluted virus at a speed of 100 nL/s.

NOTE: Air bubbles in the tube should be discharged using the control panel to guarantee that the micropipette dispenses the appropriate amount of liquid. If the liquid volume is still inaccurate after multiple tries, consider switching out the micropipette and starting over. We recommend aspirating some additional virus than the actual injection volume; this approach prevents the inadvertent injection of mineral oil into the mouse brain.

20. Move the micropipette above the craniotomy region; then, slowly move it down into the brain tissue to the targeted Z-axis of D/V: 1.70 mm below the brain surface.

NOTE: Many references atlas use the skull surface as D/V 0. In our experience, using the coordinates from the brain surface yielded more reliable targeting for DG.

21. Use the control panel to set the injector to inject 80 nL of the virus at a flow rate of 1 nL/s (**Figure 2D**). Click the **INJECT** button on the control panel to inject the virus. Subsequently, select two other positions within the craniotomy and repeat the previous operation.

NOTE: Each injection takes ~2 min. After finishing the injection, wait for an additional 8-10 min before moving to another position. When bleeding occurs during removal, wash promptly with saline.

22. Remove the micropipette out of the brain slowly (**Figure 2E**).

2. GRIN lens implantation in the dentate gyrus

NOTE: Perform this step immediately after completing the 240 nL viral injection.

1. Disinfect the 1 mm diameter GRIN lens in 75% ethanol for 20 min; rinse it properly with saline before implantation.

2. Expand the craniotomy using the microdrill to increase the opening in the A/P direction to roughly 1 mm. Clear the debris with saline.

3. Clamp the GRIN lens in place with a holder and make sure to expose an adequate length.

NOTE: It is easy to glue the holder to the GRIN lens when fixing it on the skull using UV resin in the subsequent steps. However, this can be avoided if the exposed length of the lens is adequate.

4. Use the holder to move the GRIN lens above the craniotomy region. Set the Z-axis position to zero when the bottom of the GRIN lens touches the surface of the brain tissue. Then, remove the GRIN lens holder and set it aside.

5. Attach the 25 G luer lock blunt needle to the vacuum pump suction tube and adjust the pressure to 0.04 MPa.

NOTE: If this step is performed for the first time, the pressure can be appropriately reduced to slowly aspirate the brain tissue.

6. Suction the brain tissue by revolving the tip of the blunt needle closely above the brain tissue and press gently on the brain tissue to facilitate the aspiration. Rinse with saline (store at 4 °C) continuously during suctioning to maintain a clear view of the brain. Observe the tissue features closely to monitor the depth of aspiration: the cortical tissue is pale pink, the corpus callosum underneath appears as white, fibrous tissue, and the hippocampal CA1 layer is dark red and grey. Stop the suction when the surface of the tissue becomes smooth and a large area of CA1 is exposed (**Figure 3**).

NOTE: This step is critical for the success of the entire procedure and is often the most difficult part. We have provided a list of common issues to help the

readers troubleshoot this step (**Table 1**). Furthermore, we recommend rinsing the wound continuously with cold saline, since this can reduce the bleeding to some extent.

1. If the needle gets clogged; attach the blocked needle to a syringe and wash out the blockage. Try changing the needle if this does not work.
2. If bleeding is constant, it can block the view of the brain tissue. If this happens, wait for the blood to clot, then rinse it with saline.
7. Move the holder above the drilled hole. Set the Z-axis to 0 when the GRIN lens contacts the surface of the brain tissue. If the GRIN lens exceeds the diameter of the hole, use the microdrill to expand the hole. Then, repeat this procedure.
8. Insert the GRIN lens into the hole at the D/V: -1.32 mm. Let the holder stand for 5-10 min. After raising the holder, rinse the hole with saline. Repeat this step 3x (**Figure 4A**).
NOTE: It is normal for the brain tissue to bleed during this step. After repeated saline rinses, there should be no more blood in the hole. The imaging quality is greatly affected by this step, and if the blood is not cleaned up, it may cause the imaging field to be black.
9. Use saline to clean the skull thoroughly and then let the skull dry before applying the UV resin.
10. Use a needle to apply the UV resin around the GRIN lens. Illuminate this area with a UV light for 15 s and ensure that the UV resin becomes solid (**Figure 4B**).
NOTE: Apply the UV resin a little at a time and repeat this operation several times until the area around the GRIN lens is covered. Be careful not to affix the GRIN lens to the holder when using the UV light for illumination.

11. Remove the holder from the GRIN lens carefully. Cover the entire exposed skull with UV resin and place the headplate on the skull in the appropriate position. Illuminate the entire skull and headplate with a UV light for 15 s (**Figure 4C**).

NOTE: The headplate is a component to securely hold the mouse's head in place when attaching the baseplate (see **Supplemental File 1** for the design). Secure the headplate as firmly as possible; a detached headplate will result in the failure of the entire surgery. In our experience, thorough application of the UV resin should be able to provide firm attachment. If stronger attachment is required, one could consider installing skull screws.

12. Cover the exposed GRIN lens with a 3D printed protective cap (See **Supplemental File 2** for the design). Fix the cap to the headplate using M1.6 screws (**Figure 4D**).
13. Inject dexamethasone intraperitoneally (dissolved in 0.9% saline, 2 mg/kg) after the operation to prevent postoperative inflammation. Additionally, administer subcutaneous injections of carprofen (dissolved in 0.9% saline, 5 mg/kg) to reduce postoperative pain.
14. Place the mice back in the cage and transfer them to a thermal blanket to facilitate their recovery. Then, transfer the mice to the experimental animal house after they can move freely.
NOTE: To avoid damage to the base plate by fighting, mice that have undergone the surgery may be housed individually or with a minimal number of cohabitators. We recommend not exceeding three mice in a cage after surgery.

15. Disinfect the work surfaces by using a 10% bleach solution. Remove disposable personal protective equipment (PPE) and dispose of it in biohazard bags.
16. Monitor the mice daily for 3 days after the surgery. Record mice's body weight and observe their wound healing status and locomotion activities. Provide daily intraperitoneal injections of dexamethasone and carprofen solutions (the same dosage as in step 2.13) for 3 days. Provide moist chow or treatment to facilitate recovery when necessary.

3. Check the quality of the imaging field

NOTE: The mouse recovers in 2-3 weeks after surgery before the first *in vivo* calcium imaging session. The purpose of this step is to check the quality of the surgery and the recovery of the mouse. If single-cell activity can be observed in the imaging field and the mouse is in good condition, affix the base plate to the mouse skull. The mouse should be euthanized by cervical dislocation if the imaging quality or health condition is not adequate.

1. Connect the miniscope data collection Box to the computer with a USB 3.0 cable. Then connect the Coax Cable to the Box via the **To Scope** connector (SMA).
2. Turn on the miniscope control Software. In the Software, click **Select Config File | User Configuration Files V4 plus** to view the live images.
3. Use a customized holder to retain the mouse on the running wheel by clamping the headplate. Hold the miniscope with the miniscope holder (made with 3D printing; see **Supplemental File 3** for design), and utilize a stereotaxic instrument to move the miniscope above the head of the mouse (**Figure 4E**).
4. Remove the cap with a screwdriver. Gently wipe the surface of the GRIN lens with 75% ethanol. Position the miniscope just above the exposed GRIN lens and make the bottom surface of the scope parallel to the surface of the lens. Find the best focal plane by slowly bringing the miniscope down towards the GRIN lens.

NOTE: Set the focal plane at 0, then adjust the position of the miniscope; this provides more room to adjust the focus. Select the focal plane with a clear visualization of the greatest number of cells.
5. In the miniscope control Software, adjust the LED light power to the optimal level.

NOTE: To observe single-cell activity, the imaging field should be neither overexposed nor too dark. The **LED intensity** is typically within **10%**.
6. If vascular blood flow is visible and the cells are numerous and uniformly distributed throughout the imaging field, proceed to the next section of the experiment.

NOTE: In this step, it is important to be able to observe single-cell activity. This can influence the results of the data analysis. Normally, regional activities (blobs of fluorescent fluctuations) are difficult to interpret. This may be an indication that target neurons are out of focus of the GRIN lens. The mouse will not be used in the subsequent experiments if it appears that the imaging field is black, the cells exhibit regional activity, or there are insufficient number of cells.
7. Disconnect the cable from the miniscope.

4. Attach the miniscope base plate to the mouse skull

1. Attach the base plate to the miniscope, and re-adjust the positions of the miniscope to obtain a field of view with good imaging quality.

2. Mix the denture base materials in the mixing bowl.

NOTE: It is important that the mixture neither flows too freely nor is too firm. Too much fluidity tends to cover the surface of the GRIN lens causing the loss of imaging field. If too firm, the denture base materials will not be able to tightly cover the gap between the base plate and the headplate.

3. Take care to not change the miniscope's position while applying the first layer of denture base materials around the miniscope base plate carefully. Wait for the first layer of cement to harden before applying a second layer of cement from the base plate to the headplate. After the hardening of all denture base materials, loosen the set screw and detach the miniscope from the base plate.

NOTE: When using denture base materials, pay attention to the imaging field in the software and make any necessary adjustments before the cement solidifies.

4. Remove the holding arm from the miniscope gently.

5. Put the base plate cap into the base plate to protect the exposed GRIN lens and tighten the set screw (**Figure 4F**).

6. Place the mouse back in its home cage. Give the mouse several days to recover before conducting the behavioral experiments.

5. Data acquisition

NOTE: *In vivo* calcium imaging can be performed simultaneously with any behavior tests. In this protocol, we use the linear track as an example. This linear track is 1.5 m and has water at both ends, which serves as a reward for the mice. The mice can wear a miniature microscope (miniscope) and run back and forth along the track for a duration of 20 min. During this time, the mice are typically able to run ~60 trials.

1. Connect the miniscope data collection Box to the computer with a USB 3.0 cable. Then connect the Coax Cable to the Box via the **To Scope** (SMA) connector.

2. Turn on the miniscope control Software. In miniscope control Software, click **Select Config File | User Configuration Files V4 plus** to view the live images.

3. Connect the industrial camera to the computer with a USB 3.0 cable.

4. Turn on the camera control software. In the software, click **Open Equipment**, and select the file to import the data collection parameters. Select the video format as **Uncompressed Video in AVI Container**. Click the **Start** button to view the live images.

NOTE: To decrease the file size of the behavioral recording video, the field of view should exclude any unnecessary areas outside of the track.

5. Use a customized holder to retain the mouse on the running wheel by clamping the headplate.

6. Loosen the set screw with a screwdriver, remove the base plate cap, and clean the surface of the GRIN lens with 75% ethanol.

7. Mount the miniscope to its base. Fasten the miniscope to its base on the mouse's head.
8. Find the best focal plane by sliding the focal plane button.
9. Move the mouse from the running wheel to the linear track gently.
10. Click and hold the **Record** button to begin recording with the miniscope. Next, click the **Start Collecting** button to start the camera recording. Record for 20 min.
11. Save *in vivo* calcium imaging data, behavioral data, and Arduino data separately. Name these files with date, session number, and the mouse number.
NOTE: Studies that use a miniscope tend to have a long-term data collection period on a single experimental animal. Naming the files clearly can help with the data processing procedure.
12. Detach the miniscope from its base.
13. Close the camera control software, the miniscope control software, and the computer.
14. Disconnect the coax cable from the **To Scope** (SMA) and the USB 3.0 cable from the camera.
15. Unscrew the set screw in the base, put the base plate cap back, and tighten the screw.
16. Put the mouse back in its home cage.

6. Data processing

1. Load the recorded calcium imaging data in MATLAB.
NOTE: We recognize that the analysis of the data should be tailored to the experimental design. Here we provide a preprocessing pipeline that converts the raw calcium imaging video into activity traces from individual cells. We believe this procedure is relatively universal and useful

for the users. All scripts described in this section can be found in **Supplemental File 4**.

2. Convert the imaging data from AVI to HDF5 (.h5) format.
NOTE: The raw output of the miniscope generates AVI files with compression. The uncompressed files are usually tens of gigabytes in size. The HDF5 file format allows virtual and partial access that can be easily visualized and manipulated for subsequent analysis.
3. Apply the Non-Rigid Motion Correction (NoRMCorre)¹⁹.
4. Down-sample the motion-corrected movie in case the computer is RAM limited for later steps.
NOTE: The original data collected by miniscope has a size of 600 x 600. By using a spatial down-sample, we can reduce the video size to 200 x 200. This method significantly decreases the data storage requirements and allows for faster data processing.
5. Apply EXTRACT on the down-sampled data to identify single-cell signals, following the instructions for the EXTRACT code in the online repository²⁰ (<https://github.com/schnitzer-lab/EXTRACT-public>).

Representative Results

Figure 1 shows the schematic of the experimental procedure, including virus injection, GRIN lens implantation, base plate affixation, *in vivo* calcium imaging via a miniscope, and data processing. Generally, the entire procedure takes 1 month. **Figure 2** shows example procedures of virus injection, including the positioning of the drilled hole on the skull and the condition of brain tissue before GRIN lens implantation.

Figure 3 shows the process of removing the brain tissue, which is crucial for the success of this surgery. As more tissue is suctioned, different tissue layers become visible.

This suctioning step can be stopped once a grey, reflective layer is observed.

Figure 4 shows the procedure of the GRIN implantation, including inserting the GRIN lens, adhering the headplate on the skull, and covering the GRIN lens with a customized cap.

The imaging quality of *in vivo* calcium imaging depends on the success of the virus injection and GRIN lens implantation.

Figure 5 shows four types of results from *in vivo* calcium imaging. **Figure 5A** is the unsuccessful result; no active cells were observed in the imaging field of view. **Figure 5B-D** are successful results. **Figure 5B** has fewer than 10 active cells, but there are no obvious blood vessels. **Figure 5C** has more than 50 active cells and visible blood vessels. In **Figure 5D**, there are hundreds of active cells in the imaging field of view; at the same time, we observed clear blood vessels. High-quality *in vivo* calcium imaging typically has hundreds of activated cells. Fewer than a dozen activated cells are thought to be suboptimal for imaging results. Usually, the number of cells correlates with the diameter of the GRIN lens as well as the part of the brain region. A larger GRIN lens diameter and a closer brain region to the dorsal side will increase the probability of observing more active cells. It is

also vital to note that the larger the diameter of the GRIN lens, the more damage it does to the mouse brain; thus, selecting the appropriate size is crucial. Implanting a GRIN lens of 1 mm diameter does not affect the animal's ability to acquire the linear track behavior (**Supplemental Figure S1**).

Behavioral data and calcium imaging data are usually processed separately. Mouse behavioral data can be labeled manually or processed using open-source analysis software. Calcium imaging data are processed using Non-Rigid Motion Correction (NoRMCorre) and EXTRACT in MATLAB. **Figure 6** shows the extracted individual cells superimposed on the field of view and shows five representative calcium traces from a successful *in vivo* calcium imaging recording. See **Supplemental Video S1** for a representative video of the raw data.

Verifying that the GRIN lens implantation and viral injection take place in the intended brain region is the last step and is also very important for the interpretation of the data. **Figure 7** is a mouse brain slice showing the position of GCaMP6f expression (the green fluorescence region) and the track of the GRIN lens.

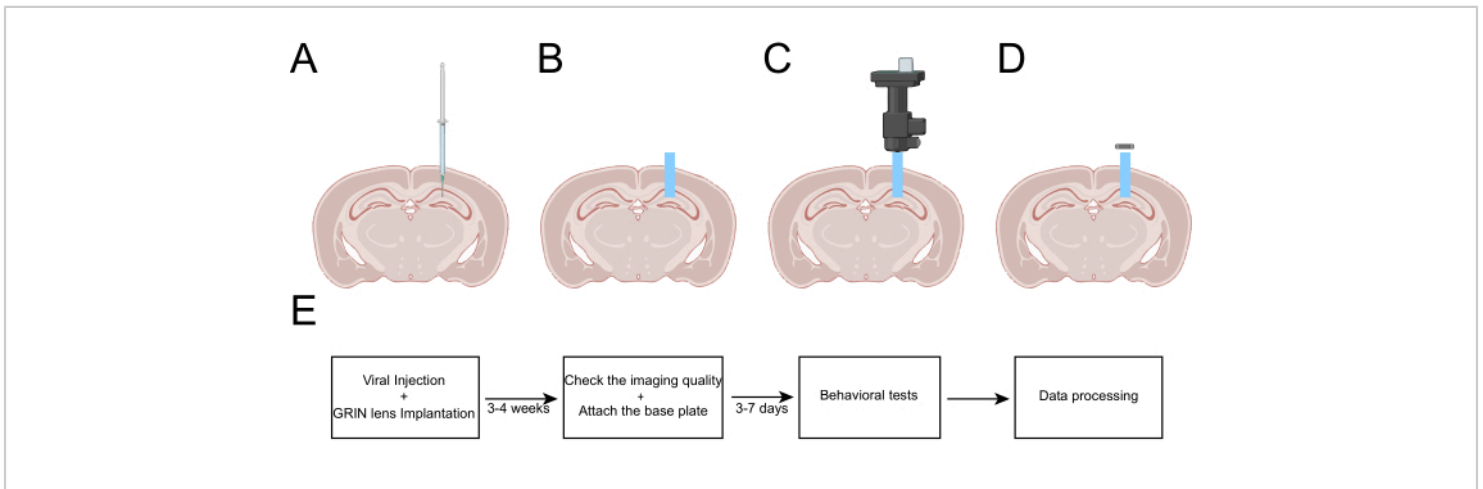


Figure 1: Diagram of the procedures of virus injection and GRIN lens implantation. (A) Inject the AAV-CaMKII α -GCaMP6f virus in the dentate gyrus. (B) Implant the GRIN lens above the dentate gyrus. (C) Check the imaging quality after surgery. (D) Affix the miniscope base plate after checking. (E) The timeline and process of the whole protocol. Abbreviation: GRIN = Gradient index. [Please click here to view a larger version of this figure.](#)

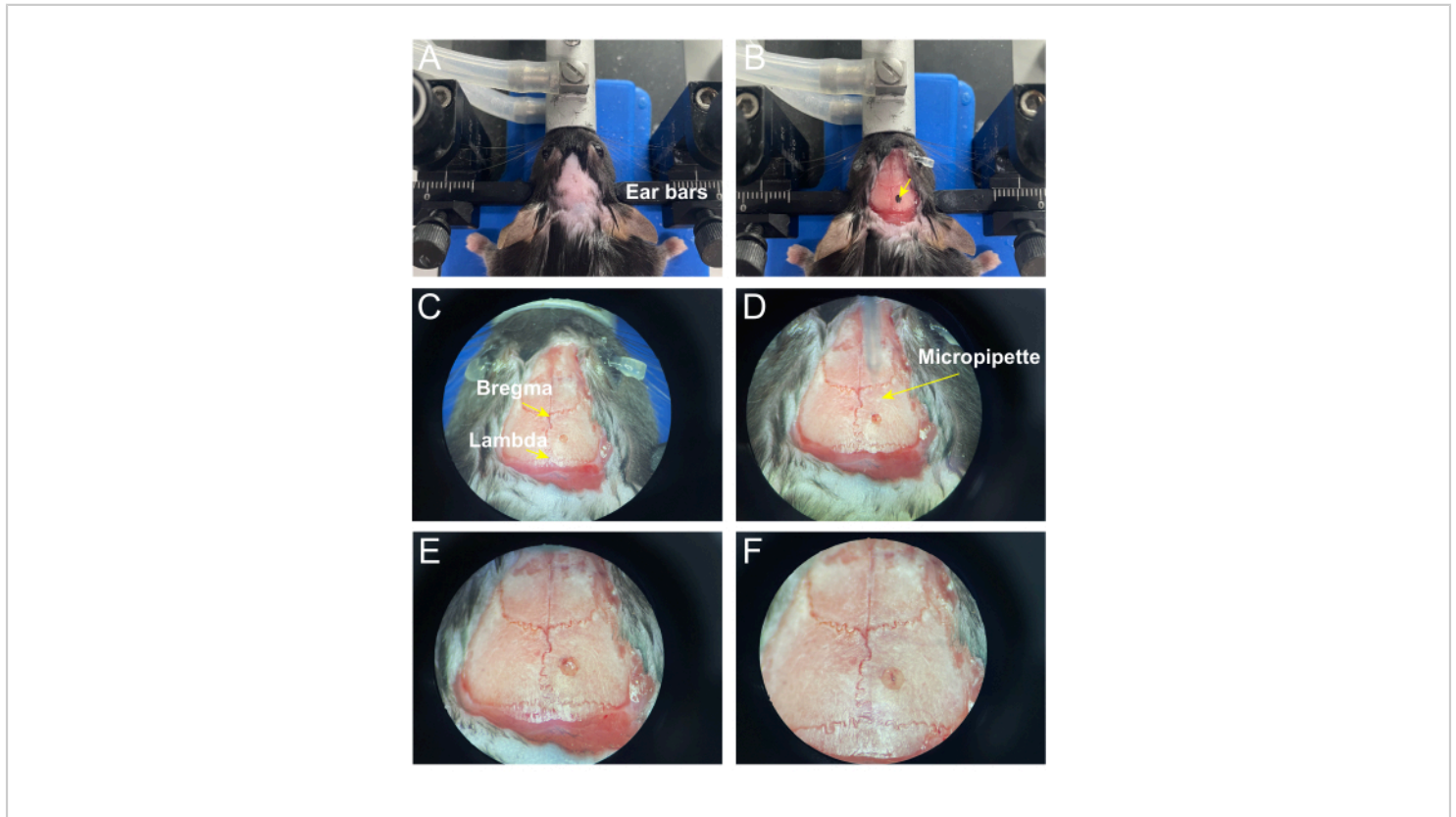


Figure 2: Representative surgical view during virus injection. (A) Place the mouse on the stereotaxic apparatus. (B) Mark the GRIN lens implantation area (the black region). (C) Craniotomy on the target area. (D) Inject 240 nL of virus into the dentate gyrus. (E) Remove the micropipette after injection. (F) Remove the cortex and part of CA1 brain tissue. [Please click here to view a larger version of this figure.](#)

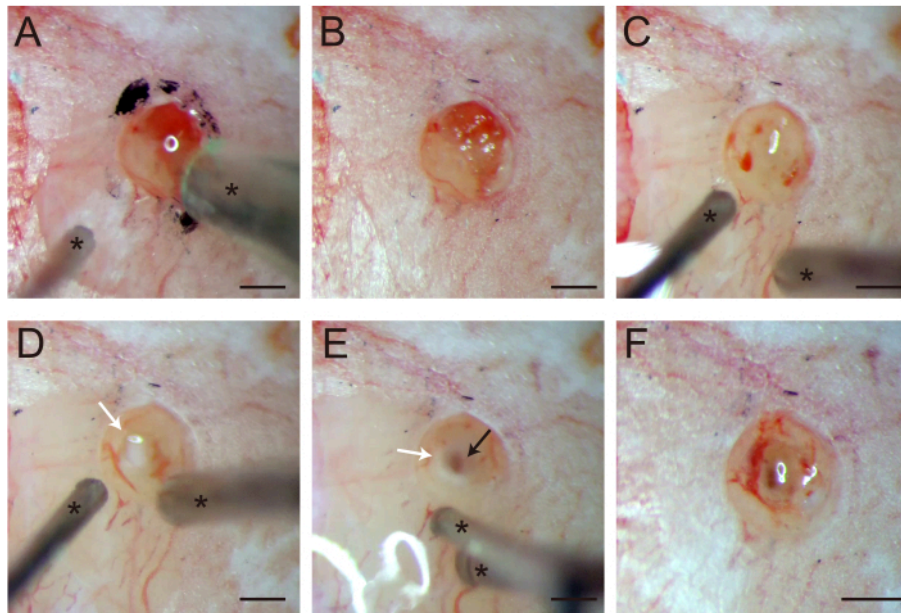


Figure 3: Representative surgical view during brain tissue aspiration. (A) The region enclosed by the black marker is polished using a microdrill, leaving behind (B) partially exposed cortical tissue. The left part shows an exposed cortex and the right part is covered by dura and skull tissue. (C) Representative image during the aspiration of the cortical brain tissue. The tissue remains pale pink. (D) White matter is visible within the field of view, as indicated by the white arrow. (E) Further suctioning revealed a dark grey-red, reflective surface underneath the white matter. The region (black arrow) is thought to be the CA1 surface and the suction should not go deeper. (F) No more bleeding is visible from the region after rinsing with saline several times. In all panels, the asterisks indicate surgical tools: a 30 G blunt needle for saline and a 25 G blunt needle for brain tissue aspiration. Scale bars = 500 μm . [Please click here to view a larger version of this figure.](#)

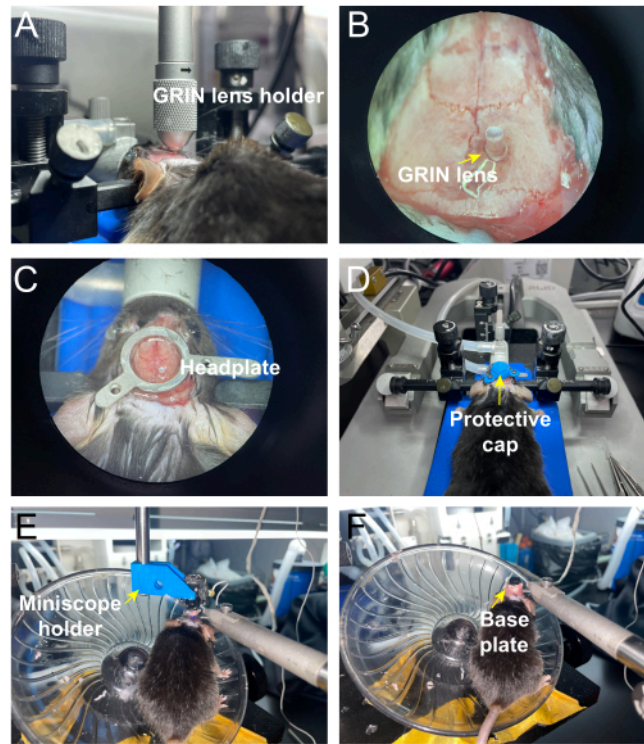


Figure 4: An example procedure for GRIN lens implantation and base plate attachment. (A) Implant the GRIN lens into the brain tissue using a GRIN lens holder. (B) Adhere the GRIN lens in the proper location with UV resin; the reflective part represents the UV resin. (C) Attach the headplate on the mouse skull using UV resin. (D) Cover the GRIN lens with a 3D printed protective cap. (E) Check the surgery quality. The miniscope was fixed by a holder. (F) Apply the denture base materials around the base plate. [Please click here to view a larger version of this figure.](#)

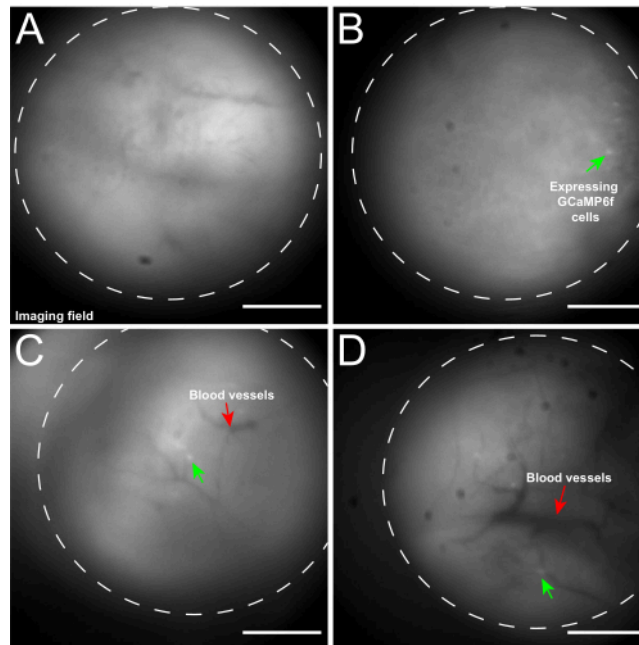


Figure 5: Successful and unsuccessful imaging results. (A) Unsuccessful *in vivo* calcium imaging result. There are no active cells in A and multiple regions have dark blood stains as indicated by the black arrows. (B-D) Successful *in vivo* calcium imaging results. (B) Less than 10 active cells can be observed but no significant blood vessels in the imaging field. (C) More than 50 active cells and significant blood vessels can be observed. (D) Hundreds of active cells and more significant blood vessels can be observed. The dashed circles represent the imaging field of view. The green arrows represent the cells expressing GCaMP6f. The red arrows represent the blood vessels. Scale bars = 250 μm . [Please click here to view a larger version of this figure.](#)

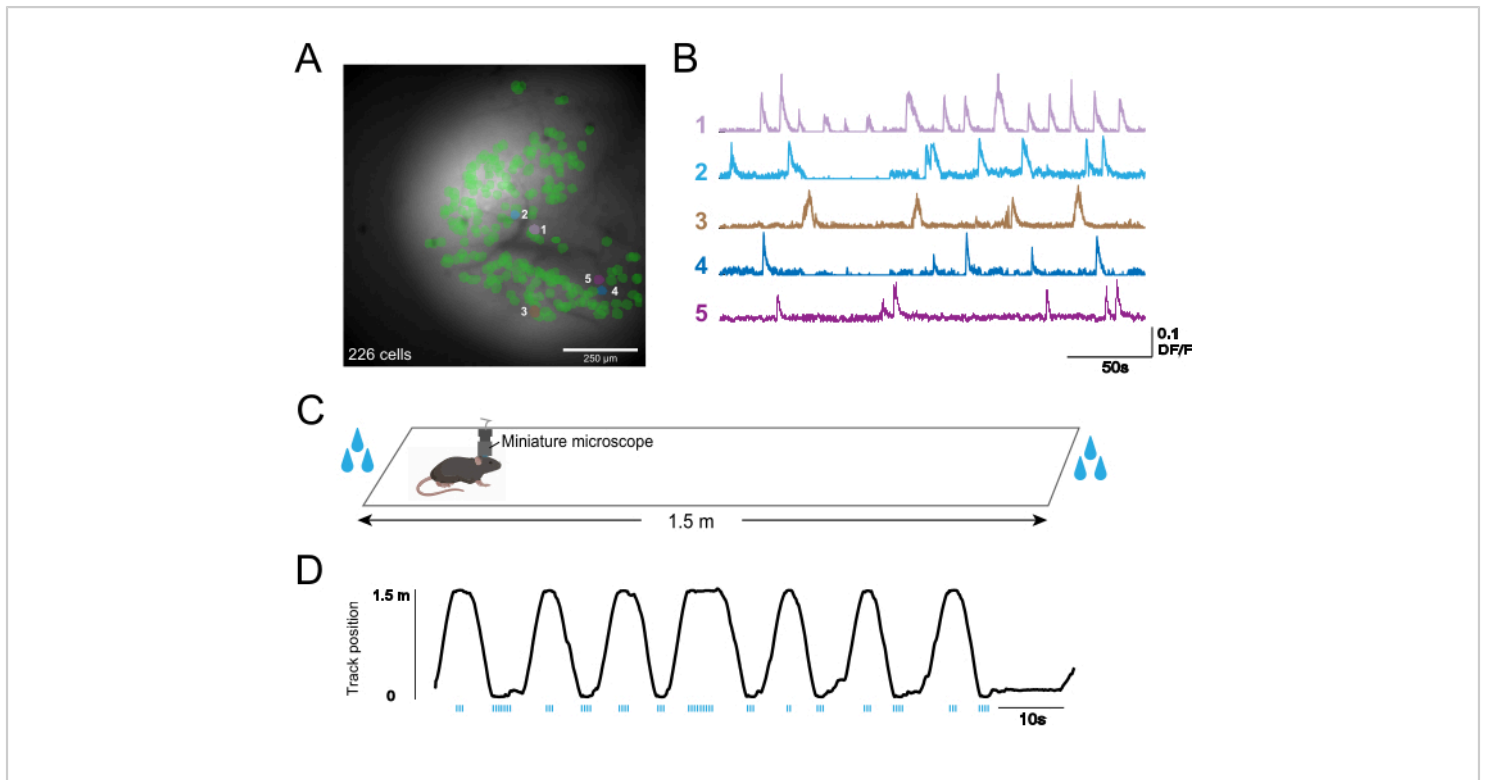


Figure 6: Representative *in vivo* calcium imaging data from a mouse running on the linear track. (A) The imaging field of view recording by the miniscope, total cell number = 227. **(B)** Representative calcium traces. The locations of the cell are shown in the same color in **A**. **(C)** Behavioral task: Linear track with water rewards at both ends. **(D)** Representative result of the behavioral analysis of the mouse's activity; total time = 100 s. Blue vertical lines indicate time points of the licking behavior. [Please click here to view a larger version of this figure.](#)

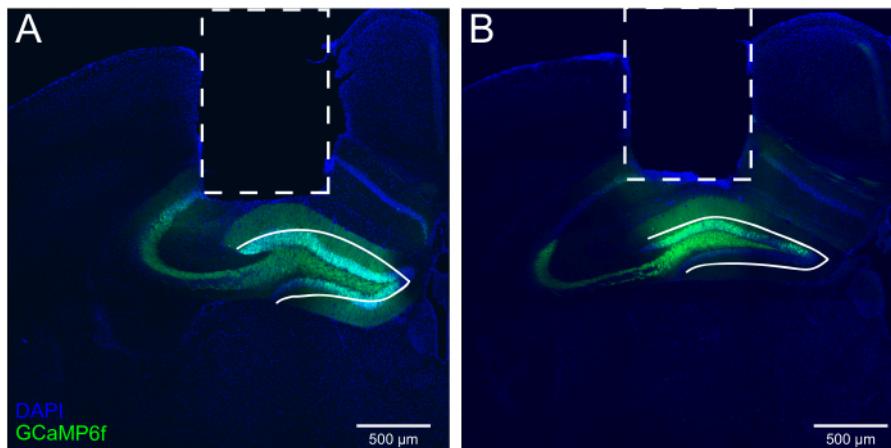


Figure 7: Brain tissue sections from mice after surgery. (A,B) Two examples of mouse brain tissues. The dashed rectangular areas indicate the GRIN lens implantation path. The curved lines represent the dentate gyrus in the hippocampus. Scale bars = 500 μm. [Please click here to view a larger version of this figure.](#)

Problem	Possible cause	Solution
The imaging field appears dark or black.	There is a significant amount of residual blood on the underside of the GRIN lens.	Prior to implanting the GRIN lens, the saline solution is used to continuously flush the surface of the surgical site until there is no longer any observable bleeding.
There are clearly visible blood vessels present in the imaging field, but no discernible neuronal activity.	1. The virus expression was suboptimal or poor.	1. It would be advisable to check the following:
	2. The location of the observed virus expression does not match the position where the GRIN lens was implanted (generally, the implantation position of the GRIN lens is too shallow compared to the desired location).	a. Ensure the virus storage conditions are appropriate.
		b. Verify the virus injection location is correct.
		c. Confirm the virus concentration is suitable.
		2. During the next surgical procedure, the depth of the GRIN lens implantation can be increased appropriately, and the exact depth should be carefully recorded each time the experiment is conducted.
The imaging field shows some regional patterns of neuronal activity, but there is no clearly visible activity at the individual cell level.	1. The volume of injected virus was excessively high.	1. Dilute the virus or reduce the volume of the virus injection.
	2. The location of the virus expression does not align with the position of the GRIN lens (typically, the GRIN lens is implanted at a shallower depth than the optimal position for the virus expression).	2. During the next surgical procedure, the depth of the GRIN lens implantation can be increased appropriately, and the exact depth should be carefully recorded each time the experiment is conducted.

<p>There are certain cells within the imaging field that maintain a consistently bright fluorescence signal at all times, and there is no change in the intensity of this fluorescence.</p>	<p>The virus is overexpressed within a single cell.</p>	<p>Dilute the virus or reduce the volume of the virus injection.</p>
---	---	--

Table 1: Troubleshooting chart. [Please click here to download this Table.](#)

Supplemental Figure S1: Normal acquisition of the spatial memory task by mice that have undergone surgery.

The graph shows the quantification of the number of completed trials in the 20 min session each day. Data are represented as mean \pm SEM. N = 3 mice in with-surgery group and 4 in without-surgery group. Two-way ANOVA was used for statistical comparison. Abbreviation: ns = not significant.

[Please click here to download this File.](#)

Supplemental Video S1: Representative raw data of calcium imaging in DG.

This video demonstrates calcium activity over a 5 min period. The video is played at 10x of the original speed. [Please click here to download this File.](#)

Supplemental File 1: The design of the headplate.

This file outlines the 2D drawing of the headplate design. The production of the headplate involves cutting of stainless steel according to the drawing. The two small holes on the sidebar should be tapped with M1.6 threads. [Please click here to download this File.](#)

Supplemental File 2: The design of the 3D printed protective cap.

This file provides the gcode of the protective cap slices that can be used with a 3D printer. In this protocol, we used polylactic acid plastic as the raw material for the printing. The small holes on the side match the positions of

tapped holes on the headplate for installation. [Please click here to download this File.](#)

Supplemental File 3: The design of the miniscope holder.

This file provides the gcode of the miniscope holder slices that can be used with a 3D printer. The cylindrical hole is used for installation to a stereotaxic holder with a M4 screw. The holes on the side are intended to add screws for tightening, but the holder can be used without this feature. [Please click here to download this File.](#)

Supplemental File 4: Arduino control code and scripts for raw calcium imaging video preprocessing.

This file contains the scripts for controlling Arduino and the code for pre-processing calcium imaging data. The Arduino code controls the behavior setup in which the mouse learns to lick for water rewards at alternating ends of a linear track. Upon learning the task, the mice will repeatedly run back and forth on the track. The calcium imaging preprocessing code performs file format conversion, motion correction, spatial down-sample, and cell signal extraction from the data collected by the miniscope. [Please click here to download this File.](#)

Discussion

Here we described a procedure for *in vivo* calcium imaging in the DG of mice. We believe that this protocol will be useful for researchers aiming to study DG functions in various cognitive processes, particularly in cases where a genetically identified subpopulation is of interest. Here we explain the advantages of our protocol, emphasizing some key points in surgery, and discuss the limitations of this method.

We have tested various procedures for DG imaging from the available literature and optimized the experimental procedures as detailed in this protocol. In our opinion, the following three key modifications greatly improved the success rate for our protocol. First, we combined all surgical procedures in one sitting, while many calcium imaging studies for subcortical regions performed virus injection and lens implantation in two separate surgeries. A key advantage of our approach is that virus expression and brain tissue recovery are now happening during the same period, reducing the waiting time for mouse preparation by half, which usually takes months²¹. Furthermore, separate surgeries require accurate re-positioning of the mouse, as slight tilts with a mismatch in the range of 100 μm will lead to failure of the procedure. To avoid misplacing the lens, some groups developed an approach that attaches the miniscope to the lens and tried to view the neuronal expression of the sensor during the implanting surgery. This workaround requires non-trivial engineering of the commonly used stereotaxic apparatus and is complex to use due to the suppression of neuron activities during anesthesia. Our method does not require re-positioning of the mouse, thereby greatly reducing the time and stress associated with the procedure.

The second key point of our approach is that we repeatedly inject small amounts of the virus into the target area²². This leads to more cells becoming infected. Importantly, compared to increasing the virus load in a single injection site, this approach yielded superior results in that the locations of infected cells spread uniformly across the field of view. Another related key point is that diluting the virus titer improves the quality of calcium imaging. In our experience, an excessive amount of virus is associated with the appearance of wave-like clusters of activities, which is consistent with a previous report²³. While we initially suspected that tissue aspiration may lead to premature clearance of the virus in the injection site and insufficient expression, we did not observe such a phenomenon, and our protocol generally yielded robust infection of the target region. Compared to transgenic mice expressing GCaMP, the virus approach is inevitably less consistent but offers more flexible use because it does not require complicated breeding. However, as the expression of the GCaMP may spill into adjacent brain structures or become unevenly distributed in the target brain region, careful examination of the anatomical positions of virus and lens from the fixed tissue is critical for the interpretation of the results. Combining region- or celltype-specific Cre lines with Cre-dependent GCaMP expression could improve the specificity of imaged signals.

The third key point of our protocol is that during the implantation of the lens, we repeated lens insertion and rinsing several times to make sure that there was no leftover blood in the implantation area. This is a key operation to facilitate tissue recovery and improve the success rate of the procedure. While the exact mechanism is not known, we speculate that lens insertion will inevitably cause some damage to the tissue, and the rinsing step would clear the bleeding associated with this damage. Otherwise, the

insertion-associated bleeding may take a long time for the brain to clear, which increases the probability of local inflammation and macrophage infiltration, both of which would reduce the optical quality. In addition, at the coordinates we provided in this protocol, we found that placing the lens a little closer to the sagittal suture usually results in an increased number of visible cells, although it is important to avoid piercing into the third ventricle. We have also provided a list of common problems for better troubleshooting of this step (**Table 1**).

The mouse has to be trained to wear the dummy miniscope prior to behavioral experiments to minimize the impact of added weight on the head. Typically, this training takes place ~3 days, with each session lasting 20 min. During the behavioral experiments, the physical condition of the mouse should be monitored regularly. The behavioral performance of the mouse will be greatly impacted by its health.

This protocol contains several limitations. First, it should be noted that calcium imaging is a surrogate of neural activity, which can be influenced by the expression of the sensors. The one-photon imaging methods using a miniscope may lead to overlapping signals from neighboring cells, which require de-mixing from subsequent analysis. In addition, our protocol involves invasive surgeries. A chunk of brain tissue is removed during the GRIN lens implantation step, usually including part of the CA1 region, retrosplenial cortex, and associative visual cortex. This is necessary due to the limitation of the imaging depth afforded by the one-photon illumination. In our observations, we did not notice any apparent behavioral deficits in the mice following the surgical procedure, neither in their general, unrestricted behaviors nor in the learning of the linear track tasks (**Supplemental Figure S1**). Alternatively, the use of automated surgical

instruments for brain tissue suction can reduce the errors associated with manual operation, thereby enhancing the precision of the surgical procedure²⁴. Moreover, our calcium imaging data in general yielded normal calcium dynamics. The effect on more complex cognitive functions needs further characterization. An alternative method for lens insertion without tissue aspiration has been described before²⁵. This is achieved by making a cut in the brain tissue along the tract of intended insertion and placing the lens directly through the opening. In our experience, this approach leads to folding or other deformations of the brain tissue along the insertion tract, which can still be invasive. The high variability of the deformation makes this approach less reliable than the protocol we described. Another potential caveat of our protocol is that the behavioral performance of the mouse is slightly impacted by the coax cable that connects the miniscope and the miniscope Data Acquisition (DAQ) Box. This is not only due to the wires coiling together after numerous turns, but also because the wire can be a distractor for the mouse during the task. Utilizing a wireless miniscope²⁶ would effectively resolve this problem.

Despite the existing limitations, we believe this methodology can be highly beneficial for researchers interested in using *in vivo* calcium imaging to study neuronal activity patterns within the hippocampal dentate gyrus. For example, this *in vivo* calcium imaging approach can be applied to investigate place cells specifically within the dentate gyrus region. This would enable the exploration of how place cells encode information across different brain areas^{10,27}. Our validation indicates that this protocol is reasonably reproducible, with high rates of success, and can be applied to different brain regions.

Disclosures

The authors declare no competing financial interests.

Acknowledgments

This work is supported by the Shanghai Pilot Program for Basic Research - Fudan University 21TQ1400100 (22TQ019), Shanghai Municipal Science and Technology Major Project, the Lingang Laboratory (grant no. LG-QS-202203-09) and National Natural Science Foundation of China (32371036).

References

1. Scoville, W. B. Milner, B. Loss of recent memory after bilateral hippocampal lesions. *J Neurol Neurosurg Psychiatry*. **20** (1), 11-21 (1957).
2. Spiers, H. J., Burgess, N., Hartley, T., Vargha-Khadem, F., O'keefe, J. Bilateral hippocampal pathology impairs topographical and episodic memory but not visual pattern matching. *Hippocampus*. **11** (6), 715-725 (2001).
3. Kandel, E. R. Spencer, W. A. Cellular neurophysiological approaches in the study of learning. *Physiol Rev*. **48** (1), 65-134 (1968).
4. Zemla, R. Basu, J. Hippocampal function in rodents. *Curr Opin Neurobiol*. **43**, 187-197 (2017).
5. Basu, J. Siegelbaum, S. A. The corticohippocampal circuit, synaptic plasticity, and memory. *Cold Spring Harb Perspect Biol*. **7** (11), a021733 (2015).
6. Gobbo, F. et al. Neuronal signature of spatial decision-making during navigation by freely moving rats by using calcium imaging. *Proc Natl Acad Sci U S A*. **119** (44), e2212152119 (2022).
7. Schuette, P. J. et al. Gabaergic ca1 neurons are more stable following context changes than glutamatergic cells. *Sci Rep*. **12** (1), 10310 (2022).
8. Daumas, S., Halley, H., Francés, B., Lassalle, J. M. Encoding, consolidation, and retrieval of contextual memory: Differential involvement of dorsal ca3 and ca1 hippocampal subregions. *Learn Mem*. **12** (4), 375-382 (2005).
9. Ognjanovski, N. et al. Erratum: Parvalbumin-expressing interneurons coordinate hippocampal network dynamics required for memory consolidation. *Nat Commun*. **8**, 16120 (2017).
10. Hainmueller, T. Bartos, M. Parallel emergence of stable and dynamic memory engrams in the hippocampus. *Nature*. **558** (7709), 292-296 (2018).
11. Yassa, M. A. Stark, C. E. L. Pattern separation in the hippocampus. *Trends Neurosci*. **34** (10), 515-525 (2011).
12. Ryan, T. J., Roy, D. S., Pignatelli, M., Arons, A., Tonegawa, S. Memory. Engram cells retain memory under retrograde amnesia. *Science*. **348** (6238), 1007-1013 (2015).
13. Manahan-Vaughan, D., Reymann, K. G., Brown, R. E. In vivo electrophysiological investigations into the role of histamine in the dentate gyrus of the rat. *Neuroscience*. **84** (3), 783-790 (1998).
14. Kim, S., Jung, D., Royer, S. Place cell maps slowly develop via competitive learning and conjunctive coding in the dentate gyrus. *Nat Commun*. **11** (1), 4550 (2020).
15. Danielson, N. B. et al. In vivo imaging of dentate gyrus mossy cells in behaving mice. *Neuron*. **93** (3), 552-559.e4 (2017).

16. Chen, T.-W. et al. Ultrasensitive fluorescent proteins for imaging neuronal activity. *Nature*. **499** (7458), 295-300 (2013).
17. Barnett, L. M., Hughes, T. E., Drobizhev, M. Deciphering the molecular mechanism responsible for gcamp6m's ca²⁺-dependent change in fluorescence. *PLoS One*. **12** (2), e0170934 (2017).
18. Ghosh, K. K. et al. Miniaturized integration of a fluorescence microscope. *Nat Methods*. **8** (10), 871-878 (2011).
19. Pnevmatikakis, E. A. Giovannucci, A. Normcorre: An online algorithm for piecewise rigid motion correction of calcium imaging data. *J Neurosci Methods*. **291** 83-94 (2017).
20. Inan, H. et al. Fast and statistically robust cell extraction from large-scale neural calcium imaging datasets. *bioRxiv*. 10.1101/2021.03.24.436279 2021.2003.2024.436279 (2021).
21. Thapa, R., Liang, B., Liu, R., Li, Y. Stereotaxic viral injection and gradient-index lens implantation for deep brain in vivo calcium imaging. *J Vis Exp*. (176), 10.3791/63049 (2021).
22. Wirtshafter, H. S. Disterhoft, J. F. In vivo multi-day calcium imaging of ca1 hippocampus in freely moving rats reveals a high preponderance of place cells with consistent place fields. *J Neurosci*. **42** (22), 4538-4554 (2022).
23. Masala, N. et al. Aberrant hippocampal Ca²⁺ micro-waves following synapsin-dependent adeno-associated viral expression of Ca²⁺ indicators. *bioRxiv*. 10.1101/2023.11.08.566169 (2024).
24. Liang, B., Zhang, L., Moffitt, C., Li, Y., Lin, D.-T. An open-source automated surgical instrument for microendoscope implantation. *J Neurosci Methods*. **311** 83-88 (2019).
25. Hsiao, Y.-T., Wang, A. Y.-C., Lee, T.-Y., Chang, C.-Y. Using baseplating and a miniscope preanchored with an objective lens for calcium transient research in mice. *J Vis Exp*. (172), e62611 (2021).
26. Barbera, G., Liang, B., Zhang, L., Li, Y., Lin, D. T. A wireless miniscope for deep brain imaging in freely moving mice. *J Neurosci Methods*. **323**, 56-60 (2019).
27. Cholvin, T. Bartos, M. Hemisphere-specific spatial representation by hippocampal granule cells. *Nat Commun*. **13** (1), 6227 (2022).